THREE-DIMENSIONAL FLAME HOLDING MECHANISM MEASURED BY STEREOSCOPIC PIV

Virginia R. Palero, Yuji Ikeda and Tsuyoshi Nakajima
Department of Mechanical Engineering
Kobe University, Rokkodai, Nada, Kobe 657-8501,Japan
palero@ms-5.mech.kobe-u.ac.jp
ikeda@mech.kobe-u.ac.jp
nakajima@mech.kobe-u.ac.jp

Joshep Shakal
TSI Inc. Laser Diagnostics Division
St. Paul, Minnesota, USA
jshakal@tsi.com

ABSTRACT
The three-dimensional flame holding mechanism in a gun-type burner has been investigated as well as the fuel droplet dynamics. This gun-type burner forms a recirculating swirling flow with a complex structure, essential for understanding the flame holding mechanism. The swirl flow will increase fuel-air mixing, improve flame stabilization and prevent flame attachment on the baffle plate. The central plane of the burner has been analyzed by means of Stereoscopic PIV. That technique allows the measurement of the full three-dimensional velocity vector map in a fluid plane. A complex swirl motion has been founded for the reacting condition, with the formation of a couple of twin vortex in the shear flow region that is bordering the recirculation areas. The influence of the incoming airflow velocity has been studied, founding the strongest effect on the axial and radial components, with changes in the reversing flow structure, but almost no influence on the swirl component.

INTRODUCTION
Turbulent recirculating flows are now receiving considerable attention because of their relevance in practical combustors. Of particular importance in those flows is the recirculation zone because of its complex flow pattern and its vital role in stabilizing the flame to the burner. Advances in combustion modeling and in diagnostics capabilities have encouraged researchers to study such flows both with numerical and experimental investigations.

In these last years diagnostics have developed quickly as a result of the improvement of the computers, lasers and CCD arrays. No intrusive optical diagnostics have been proved the most suitable since flow field is easily disturbed. Laser interferometric techniques such as Laser Doppler Velocimetry (LDV) (Durst, 1975) and Phase Doppler Anemometry (PDA) have already been extensively used in such environments (Edwars, 1991) for the characterization of the disperse phase. But these are point-measurement techniques and therefore do not provide any spatial information about the flame.

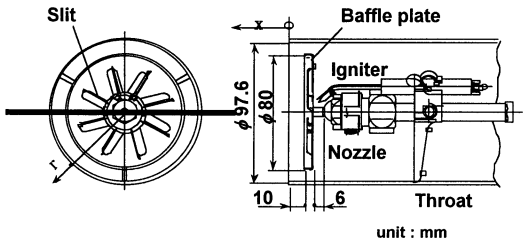

Figure 1 Gun-type burner

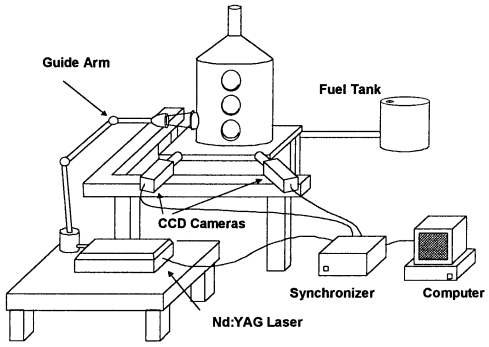

Figure 2 Experimental set-up

Figure 3: Direct flame image

On the other hand, laser spectroscopic techniques as Laser induced fluorescence (LIF) (Buschman et al, 1996) have been recently adapted to combusting sprays. That technique becomes a very powerful tool to visualize the OH/CH/C2 reaction zone and its time evolution and can provide 2D information on flame shape and flame front structure.

Another planar optical technique widely used for flow field velocity measurements is Particle Image Velocimetry (PIV), (Adrian et al., 1997, Raffel et al, 1998). That technique has some disadvantages as low data rate or particle number density, but in spite of those PIV is currently used for the diagnostic of complicated flows showing good performance.

In this work we are interested in studying the characteristics of a gun-type burner (figure 1). It is an oil burner commercially available for rather small (0.1 MW class) industrial furnaces and boilers. There is a baffle plate that serves as a flame holder and aids in reducing soot formation. The air passing through the slits will produce swirl movement. The swirl is produced in order to increase fuel-air mixing and to improve flame stabilization. As swirl is introduced in the flow, the tangential component of the swirling flow enhances the turbulent mixing of fuel and air and swirl-induced recirculation stabilizes the flame.

Initial experiments in this system were done by PDA (Kawahara et al., 1996) under isothermal and reacting conditions, and droplet behavior was described by size-classified PDA measurements (Kawahara et al., 1997). Under both conditions, it was found that small droplets (under 30 μm in diameter) entrained the recirculation area near the baffle plate, while larger droplet (bigger than 50 μm) penetrated the airflow due to their large momentum.

PIV has also shown significant applicability to spray in both conditions (Ikeda et. al, 1998, 1999). It has been found that optimised PIV optics can detect the velocity of medium size droplets (20-50 μm) in complex spray burners. As the flow is three-dimensional, PIV does not provide the complete velocity vector map. Furthermore, the out-of-plane component is a source of error in the in-plane components. There is different possibilities for measuring the out-of-plane component but the most straightforward is to apply Stereoscopic PIV (SPIV). SPIV is an extension of PIV that allows the measurement of the three-dimensional velocity vector map in a whole fluid plane (Gauthier and Rietmuller, 1988). It is based on a stereoscopic viewing of the fluid plane. The velocity vector is projected onto the direction of visualisation and differences in both projections will provide the three velocity components.

This technique has been successfully applied to the gun-type burner in non-combusting condition (Palero et al, 2000, a, b). The results were compared with PDA (SMD and size-classified) showing good agreement for the three velocity components and providing a reliable description of the three-dimensional flow structure inside the recirculation flow areas.

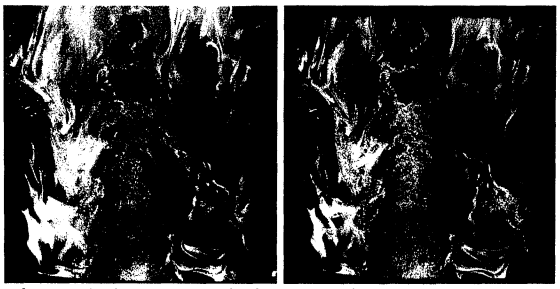

Figure 4: Stereoscopic image pair

In this paper, SPIV was applied to the combusting spray flow in order to characterise the three-dimensional structure of the flame holding mechanism. For this purpose the results obtained for reacting and non-reacting condition will be compared and discussed. A second experiment has been done by changing the velocity of the incoming airflow for the study of the changes in the recirculation zone structure.

EXPERIMENTAL SET-UP

In Figure 2 the experimental set-up for this experiments is shown. Heavy oil (type A, Japanese Industrial Standard) is pressurized up to 0.7 MPa and a hollow cone spray is produced with a 60° included angle (hollow-cone nozzle: Danfos, type H). Figure 3 shows a direct picture of the flame produced by the burner (Ikeda et al., 1995). There are three main regions: one is the flame-holding region near the baffle plate, the second is the transparent region where the fuel droplets are evaporating, and the last one is the main combustion region containing much soot luminescence.

In these experiments, a dual-cavity Nd:YAG laser (SP PIV-400, 400 mJ pulse, 532 nm) was used for illumination. Two CCD cameras (TSI PIVCAM 10-30, cross-correlation, 1000x1016 pixels, Kodak ES1.0) were used with a 60 mm focal length Micro Nikkor lenses.

Here, the stereoscopic angular method has been applied. In order to have the whole fluid plane in focus the Scheimpflug condition has been applied, by rotating the lens to a certain angle. Thus the lens can operate with the same apertures settings as the 2D PIV. The Scheimpflug camera arrangement introduces perspective distortion to the images, causing a rectangle in the light sheet plane to be imaged as a trapezoid on the image sensor. This effect is important when big stereoscopic angles and big magnification are used, meaning that the image magnification is not uniform. In this case this effect is negligible. The stereoscopic angle (α)

used for the combustion experiments was 11° (22° between both camera axes) as the test rig does not allow wide stereoscopic angles. The viewed area was 90x84 mm^2 (spatial resolution of 11.1 pixels/mm in the radial (OY) direction and 12.1 pixels/mm in the axial (OX) direction). The experimental parameters for the image recording and processing are listed in the Table 1.

	α	*f/#*	*Interrogation Area*
Cold flow	*22.5°*	*2.8*	*16x16*
Comb. flow	*11°*	*11*	*32x32*

Table 1: Parameters for the image recording and processing

Figure 4 shows the typical images recorded with this SPIV set-up. In these images, it is possible to observe different light scattering characteristics, depending on droplet size. In the central region, the image of the unburned droplets presents more intensity in the right image than in the left image. This is because for the size range of the fuel droplet (typical diameter bigger than 5 μm), forward scattering is stronger than in backward scattering. On the other hand, side regions present stronger intensity in the left image than in the right image. This strong luminescence comes from very small particles (evaporating droplets, soot particles), for which back scattering is stronger that forward-scattering. It is beyond the scope of this work to make a detailed study of light scattered by particles but it is interesting to point out that in PIV recordings size information is clearly displayed, and this subject will be investigated in future works.

Recorded images were analyzed using the cross-correlated subregions of frame-straddle images. 3D vector maps are computed by interpolating the two 2D vector fields in a new grid created to define the locations where the 3D velocity is desired. In that case the 3D-grid spacing was 2 mm. For reacting condition, that was 45x45 vectors, interpolated from 60x60 measured vectors in each stereoscopic image (interrogation area: 32x32 pixels, 50% overlap). For the non-combusting condition a super-resolution algorithm (Hart, 1999) was applied in the analysis of the images, using a final interrogation window of 16x16 pixels.

RESULTS AND DISCUSSION

For the first experiment, 450 image pairs have been recorded in reacting and non-reacting condition. In general, it is possible to have good measurements of the unburned droplet velocities, but it is not easy to know the characteristics inside the recirculation zone, as there is contribution of small evaporating droplets and soot particles.

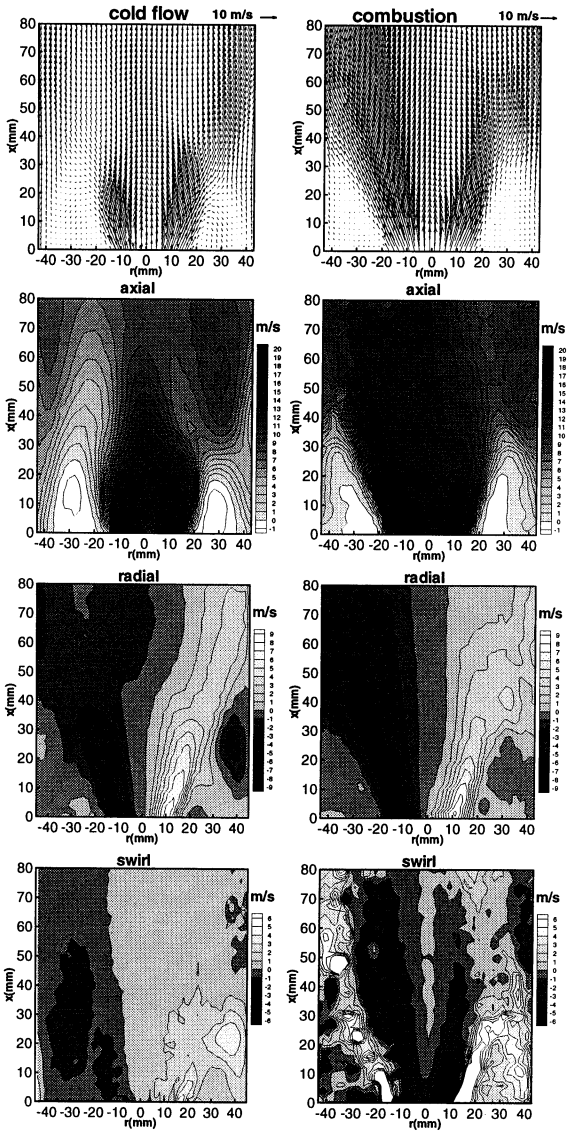

Figure 5 Averaged velocity vector maps and velocity component contours for non-reacting and reacting condition.

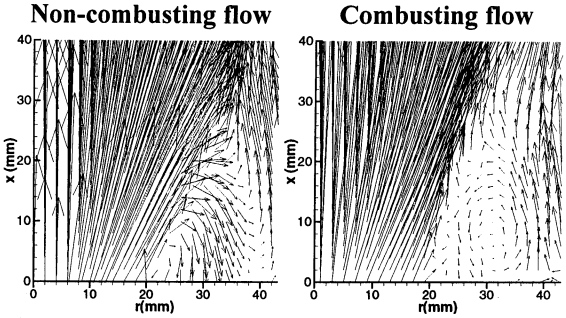

Figure 6 Recirculation zones (magnified)

In figure 5 the averaged velocity vector maps (450 samples) as well as the velocity components contours measured for non-combusting and combusting flow are compared. In the vector maps the cone structure can be easily seen. It is possible to distinguish three main areas: the centre of the

plane is the area where droplets move with high velocity. Then, the shear flow region, where the droplet velocity changes quickly. There, unburned droplets have a strong penetration, stronger in the combusting case, due to the thermal expansion. Finally at both sides of the plane, there are two recirculation areas.

The characteristics of the recirculation areas are better displayed on the velocity contour maps. In the axial component contours, we can see how the location of these areas is the same for cold and combusting flow. They start at $|r| \approx 20$ mm and their bases cover the same radial distance, about 15 mm. But while in the cold flow, they tend to expand, for the combusting flow the opposite happens. The area covered by the recirculating flow is smaller and also the velocity inside those areas, because of gas expansion.

This can be seen also in figure 6, where the recirculating zones have been magnified. In non-combusting flow, the temperature is constant all over the region, while in combustion there is an important temperature gradient across the plane. That means that the difference in the velocity will increase in the limits between the shear flow region and the reversing flow. At the same time, the pressure in the reacting recirculating zone will decrease, helping to the formation of vortexes.

For the radial component there are also some differences between both conditions. The shear in the velocity is much more important for the combusting case, even if the position of those areas is the same. This is indicating that the spray injection depends only on the injector characteristics and not on the particular working condition.

The swirl component is the one that presents the most interesting results here. Quite different behaviour was obtained for both cases. For non-combusting condition a rotating vortex is measured. The maximum swirl velocity (in absolute value) is measured in the area that limits both recirculating flows. In combustion, the structure of the swirl component is much more complicated. The recirculation zones have some moderated, not too high swirl movement coming from right to left. But in the shear flow region we can see the formation of twin vortex with the characteristic that the swirl velocity is near zero in the same narrow region where the radial component indicates the maximum shear.

Then the vorticity maps are examined (figure 7) finding again that for the combusting flow a couple of twin vortex is formed which location is the same as the vortex in the swirl component indicating that the flow has a very complicated three-dimensional structure.

For a quantitative comparison between non-combusting and combusting flow, in figure 8 the three velocity components and their corresponding rms, inside the recirculation area (x = 6 mm) are plotted. Axial and radial show the same tendencies for both cases, although they present higher values in the central and shear flow region for the combusting case. However the intensity of the recirculating flow is stronger for the non-reacting condition.

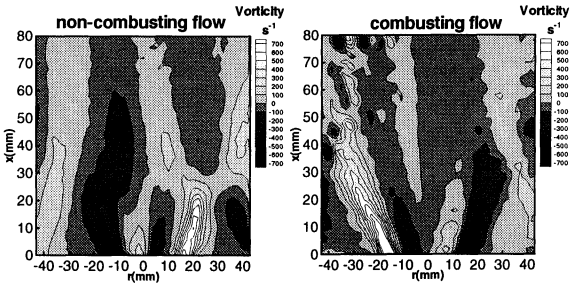

Figure 7 Vorticity maps

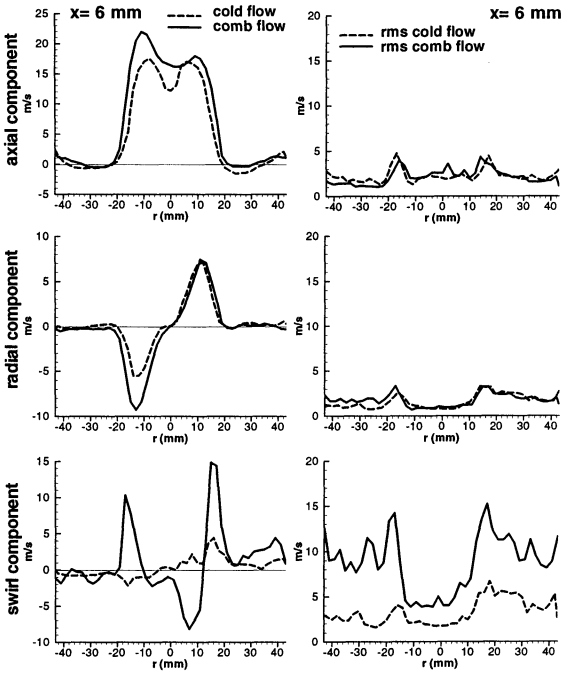

Figure 8 Velocity components and rms for non-combusting and combusting flow (x = 6mm).

The swirl velocity profiles show a complete different behaviour. Although non-combusting flow has a smooth, moderate profile, the combusting flow has strong peaks in the centre and shear flow region. It is interesting to point out that in the recirculation areas the values measured for both conditions are quite similar.

In the second experiment, the velocity of the incoming airflow was changed in order to test the effects in the flow structure, mainly on the flame holding region. The airflow rate is constant (0.0113 m^3/h) but it is possible to control its velocity by changing the diameter of the entrance pipe. Up to now, all the experiments in that furnace has been done with an incoming air velocity 3.2 times bigger than the minimum velocity (v_{min} = 2.25 m/h). This

is the condition used for the previous study here. Two more conditions have been examined here: $6.4v_{min}$ and $2.5v_{min}$.

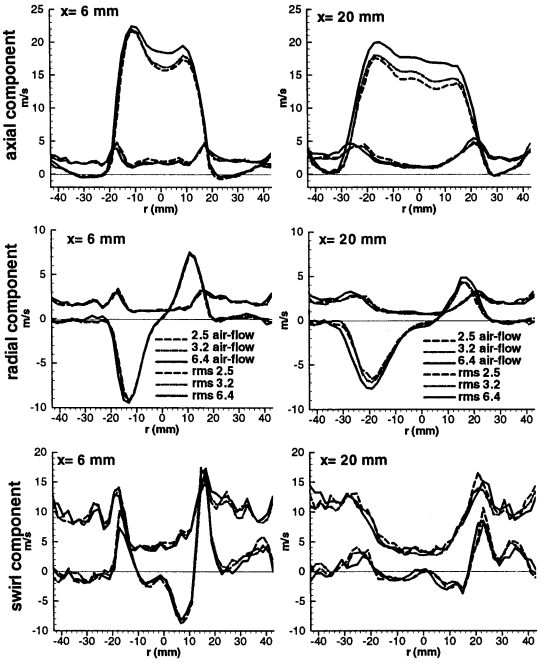

Figure 9 Velocity components and rms measured for different incoming airflow velocity at x= 6 and 20 mm.

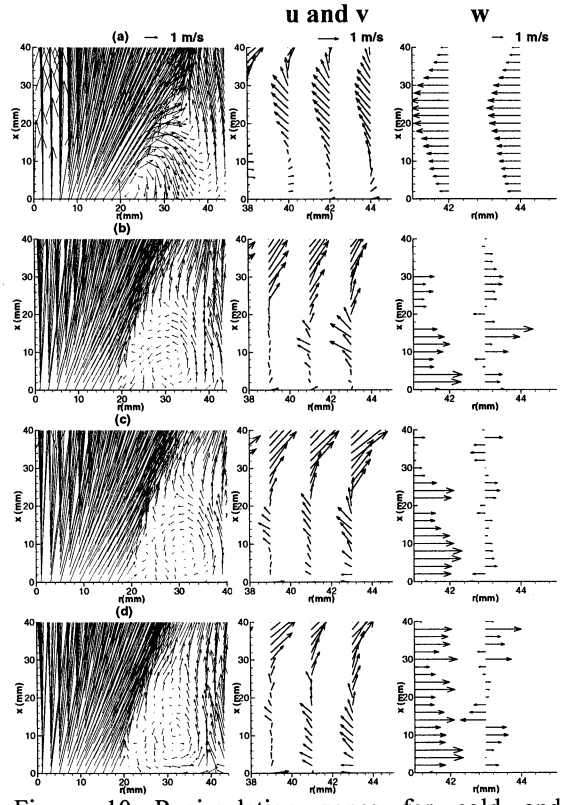

Figure 10 Recirculation zones for cold and combustion zones

In figure 9 the three velocity component are compared at two locations: inside the recirculation zone (x = 6 mm) and in its limit (x = 20 mm). As the velocity increases the axial and radial values also increase, but only in the central and shear regions.

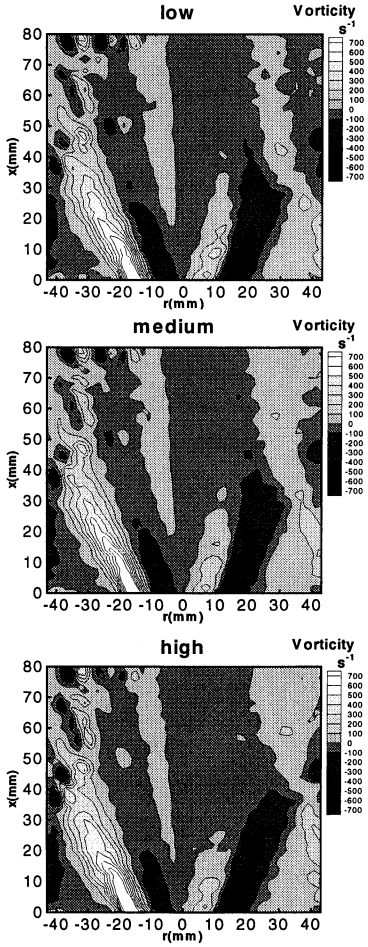

Figure 11 Vorticity contours for the three air conditions in combusting flow

For the axial component the change in the central area is ~10% of the maximum measured velocity, while the increment in the radial component is ~5%. However, the change in the air velocity introduces random fluctuations on the swirl component, and it is difficult to find any clear tendency.

The differences in the reversing flow inside the recirculation areas due to the air velocity can be seen in figure 10. Here, in the left column we are representing the right recirculation zone for non-combusting (a) and combusting flow (b ($2.5v_{min}$), c ($3.2v_{min}$) and d ($6.4v_{min}$)). On the right column a close-up of the border velocity vectors is shown. As the air velocity increases it is possible to see how one vortex is forming (b), then is completely developed in (c) whereas in (d) is starting to break in two vortexes. It is also important the contribution of the entrainment air that increases as the air velocity is larger (u and v vectors). However, not such behaviour can be seen for the non-reacting flow, where the entrainment air is not entering the recirculation zone. For the swirl component (w

vectors), the swirl increases near the recirculation zone but in the edge the swirl structure does not present any definite tendency.

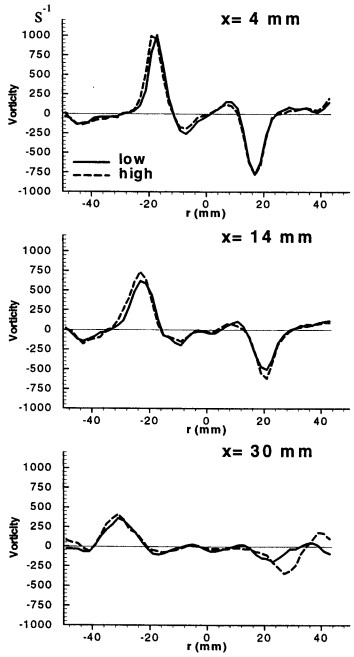

Figure 12: Vorticity lines for two incoming air conditions (high and low velocity)

The vorticity maps (figure 11) has been examined as well as the vorticity values at several locations along the spray axis (figure 12) but not significant differences have been found.

CONCLUSIONS

In this work the three-dimensional flame holding mechanism of a recirculating swirling flow has been studied. Comparing with the non-combusting flow, a complex swirl motion has been founded for the combusting flow. A couple of twin vortex is formed in the shear flow region that is bordering the recirculation areas. Those areas are smaller than in the non-combusting condition due to air entrainment and thermal expansion. The flow inside those areas presents clear vortexes that can not be seen for the non-combusting flow.

The influence of the incoming airflow velocity has been studied, founding the strongest effect on the axial and radial components, with changes in the reversing flow structure and in intensity of the entrainment air.

ACKNOWLEDGEMENTS

This research was partially supported by JSPS (P.99048, Dr. V. Palero)

References

Adrian, R.J et. al., "Developments in laser techniques and fluid mechanics", Springer Verlag, 1997

Buschman, A., Dinkelacker, F., Schäfer, M. and Wolfrum, J., *Proc. Combust. Inst.* 26, 437-445, 1996.

Durst, F. et al., "Laser Doppler measurements in two-phase flows". *Proc. LDA symposium,* Copenhagen, pp 403-429, 1975

Edwars. C.F, "Structure of a swirl-stabilized spray flame by imaging, Laser Doppler Velocimetry and Phase Doppler Anemometry", *23rd International Symposium in Combustion*, pp 1353-1359.

Gauthier,V. and Riethmuller, ML., "Application of PIDV to complex flows: measurement of the third component", VKI Lecture Series on Particle Image Displacement Velocimetry, Brussels, 1988.

Hart, D., "Super-resolution PIV by recursive local-correlation", *Journal of Visualisation*, 10, 1999.

Ikeda, Y. et al, "Flux measurements of O_2, CO_2 and NO in an oil furnace", *Meas. Sci. Technol.*, 6, 826-832, 1995.

Ikeda, Y. et, al, "PIV application for spray characteristic measurement", *Ninth. Symp. on Applic. of Laser Techniques to Fluid Mech.*, Lisbon, 1998.

Ikeda, Y. et al, "Spatial structure of a combusting spray by PIV", *First Int. Symp on Turbulence and Shear Flow Phenomena,* 1999.

Kawahara, N. et al., "Size-classified droplets dynamics of combusting spray in 0.1 Mw oil furnace", *Eighth Symp. on Applic. of Laser Techniques to Fluid Mech.*, Lisbon, 1996.

Kawahara N., Ikeda, Y., and Nakajima T, "Droplet dispersion and turbulent structure in a pressure-atomized spray flame", AIAA, paper 97-0125, 1997.

Palero, V. et al, "Comparison of PIV and SPIV in Application to Industrial Spray Burner", *10th Symp. on Applic. of Laser Techniques to Fluid Mech., Lisbon*, Portugal, 2000.

Palero. V. et al, "Stereoscopic particle image velocimetry evaluation in a spray", *Eight International Conference on Liquid Atomization and Spray Systems*, Pasadena, US, 2000.

Raffel, M., et al, "Particle Image Velocimetry, a practical guide", Springer Verlag, 1998.